

# Platform Technologies for Directly Reconstructing 3D Living Biomaterials

Suwan N. Jayasinghe,\* Jensen Auguste, and Chris J. Scotton

The techniques of electrospraying and electrospinning have existed for at least a century.<sup>[1,2]</sup> Both these approaches employ a high voltage applied to a needle accommodating the flow of media, placed above a counter electrode which could either be grounded or have an opposite charge to the needle—thus introducing the charged media to an electric field. Due to the potential difference between the two electrodes, charged media, on entering the electric field, accelerates toward the oppositely charged or grounded electrode; depending on the electrode setup and the media properties, this results in the formation of a stable cone and jet at the needle exit point, with the subsequent formation of either a spray plume of droplets (electrospraying) or a continuously elongating thread (electrospinning).

Both these approaches have been investigated in many areas of research and development, particularly with regard to paint sprays, for agricultural applications (through research into aerosol sciences), and in the filtration industry.<sup>[3]</sup> These endeavors have demonstrated the wider applicability of these technologies and hence in the last 20 years or so have been used for the direct handling of a wide range of materials, including bio-inspired materials.<sup>[4–6]</sup> These investigations have generated much interest in areas such as the development of fine monolayered surfaces, as well as the fabrication of scaffolds, which could be used for many laboratory-based fundamental biological studies.<sup>[7–9]</sup> Despite numerous publications in the literature, architectures generated with these techniques have significant technical limitations, which in our opinion have restricted their true translation into the biological and medical fields of research and development.

In 2005, Jayasinghe et al. began investigations into both electrospraying and electrospinning of immortalized cell lines.<sup>[10–12]</sup> Despite the high voltages involved, these cells were surprisingly found to be viable post-electrospraying/electrospinning; this is due to both these techniques exploring high voltage DC supplies, while applying very low currents (generally in the nA range).<sup>[4,6]</sup> Subsequent work has extended these studies to a wide repertoire of different cell types, both murine and human, immortalized or primary, stem cells, and even whole fertilized embryos from model organisms.<sup>[13–18]</sup> Well-established protocols (such as flow cytometry, genetic/genomic interrogation, and microarray analysis) demonstrated that cells processed using either electrospraying or electrospinning were indistinguishable from controls. Hence these technologies, now widely referred to as bio-electrospraying (BES) and cell electrospinning (CE), have become platform technologies for the biological and life sciences, and are undoubtedly the leading technologies for the direct handling of cells—both for distribution of cells with pinpoint precision as cell-bearing droplets, and for the formation of truly 3D living scaffolds.

Many previous studies, including our own, have been carried out with processed cells suspended in matrices generated from animal/tumor-derived materials, which contain largely uncharacterized growth factors and bioactive signals.<sup>[19]</sup> This makes them highly undesirable for clinical assays. While not applicable to humans, they have given confidence to pursue this technology with advanced biopolymers, which could be directly translated to humans, thus ensuring the potential for creating artificial constructs which could be used for a variety of applications in the regenerative medicine field. The present study describes the *in vivo* application of such biopolymers, using murine macrophages to interrogate biocompatibility and cellular behavior post-transfer.

Bio-electrospraying was carried out at various applied voltages to flow rates for the given electrode setup. A wide operational space was investigated to identify which operational conditions gave the most stable BES conditions. During these studies the selected hydrogels studied in these investigations were found to only be able to form jets, which subsequently underwent jet breakup to form charged cell-laden droplets. Hence for cell electrospinning these hydrogels were modified with the addition of laminin, which increased their viscosity in turn giving rise to the formation of an elongating cell laden fiber(s). In both scenarios, several composite cellular samples were collected and prepared for (1) cell analysis and (2) animal studies.

In these experiments, flow cytometry was used to classify cellular populations into four categories (namely: live, early apoptotic, late apoptotic, and dead), based on the binding of Annexin V and/or propidium iodide (PI) to the luciferase-transduced murine (IC-21-Luc) macrophages. In the case of apoptotic cells, the membrane phospholipid, phosphatidylserine (PS),

Dr. S. N. Jayasinghe  
BioPhysics Group  
Institute of Biomedical Engineering  
Centre for Stem Cells and Regenerative Medicine  
and Department of Mechanical Engineering  
University College London  
Torrington Place, London WC1E 7JE, UK  
E-mail: s.jayasinghe@ucl.ac.uk

J. Auguste  
Olaf Pharmaceuticals  
Biotech Three  
One Innovation Dr, Worcester  
MA 01605, USA

Dr. C. J. Scotton  
Institute of Biomedical and Clinical Science  
University of Exeter Medical School  
St Luke's Campus  
Magdalen Road, Exeter EX2 4TE, UK

This is an open access article under the terms of the Creative Commons Attribution License, which permits use, distribution and reproduction in any medium, provided the original work is properly cited.

DOI: 10.1002/adma.201503001



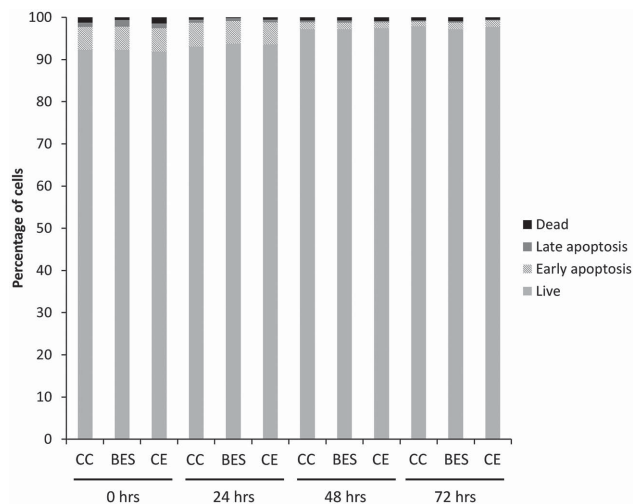


**Figure 1.** Cell viability analysis following bio-electrospinning and cell electrospinning. To confirm the anticipated benign nature of bio-electrospinning and cell electrospinning (as evidenced by extensive previous studies), a pilot flow cytometric analysis of Annexin V and propidium iodide binding was performed on macrophages up to 72 h post bio-electrospinning (BES) or cell electrospinning (CE), versus culture controls (CC). No difference in viability was observed between BES, CE, or CC at any given timepoint.

is translocated from the inner to the outer layer of the plasma membrane, allowing high affinity binding of Annexin V. In the late stages of cell death, the cell membrane loses integrity and becomes leaky to the vital dye PI, thus giving a clear and accurate measurement of the dynamics of cell death. In agreement with our extensive previous studies,<sup>[10–18]</sup> no detrimental effects of bio-electrospinning or cell electrospinning were observed over a 72 h period, in comparison with cell culture controls (abbreviated to “CC”; **Figure 1**).

IC-21-Luc macrophages (CC or BES) were then incorporated into a fluid mixture containing one of three alternative rat-tail collagen-based hydrogels, namely, CollaGel Hydrogel, CollaGel Hydrogel Soft, or CollaGel Hydrogel Soft+ (resulting in six possible combinations of macrophages and biopolymer), prior to subcutaneous injection into the shaved dorsal flanks of C57Bl/6 mice. In vivo bioluminescence was tracked longitudinally from day 1 to day 4 post-injection using an IVIS Lumina II imaging system (**Figure 2**), as described in the Experimental Section. Kinetic analysis of luminescence after intraperitoneal injection of D-luciferin highlighted that a timepoint around 25–30 min was optimal for detecting the plateau phase of luminescence (**Figure 3A**). Peak radiance declined significantly over the course of the experiment, suggesting that IC-21-Luc cells were not retained at the site of implantation. However, no significant differences in peak radiance were observed between any of the six experimental groups at a given timepoint (**Figure 3B** and **Table 1**). By recombining the data, it was apparent that implantation of either CC or BES/CE macrophages demonstrated a comparable decline in bioluminescence over time, when disregarding any effect of the biopolymer (**Figure 3C**). In contrast, analyzing any effects of the biopolymer alone, demonstrated that CollaGel Hydrogel maintained a higher peak radiance (particularly at day 3)

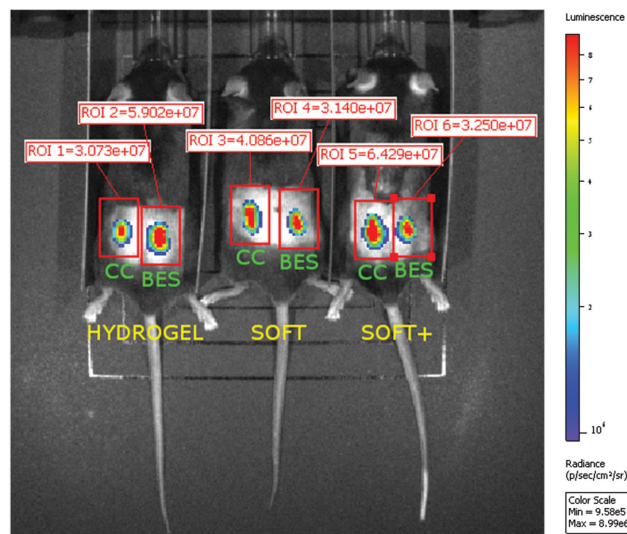


**Figure 2.** Bioluminescent imaging of implanted macrophage–biopolymer mixes. IC-21-Luc macrophages (CC or BES) were mixed with biopolymer (Hydrogel, Soft, or Soft+) and subcutaneously injected into the dorsal flanks of C57Bl/6 mice (three mice per hydrogel, with CC on the left flank and BES on the right). Following intraperitoneal injection of D-luciferin, macrophage bioluminescence was detected using an IVIS Lumina II imaging system. A representative image from day 1 post-implantation (and 25 min post luciferin injection) is shown, indicating the peak detectable radiance (photons  $s^{-1} cm^{-2}$ ) in identically sized regions of interest. The CE results were very similar to the BES implants.

compared with Hydrogel Soft or Hydrogel Soft+ (**Figure 3D**). These results highlight that subtly different cell/biopolymer combinations nevertheless have differing ability to retain cells at the site of implantation—which may be due simply to the physical nature of the biopolymer, or alterations in the microenvironmental response to the biopolymer (including local production of cellular growth factors and/or chemoattractants). Such considerations will be the topic of future investigations.

On day 4 post-injection, the tissue region incorporating the implantation site was dissected out and used for histological and immunohistochemical analysis. The gelled biopolymer was discernable in the subcutaneous region by both standard hematoxylin & eosin (H&E) staining (**Figure 4**) and a modified trichrome (MSB) stain (**Figure 5**), which labels collagen in blue. The MSB staining highlighted the dense, mature collagen in the epidermis (dark blue staining), in contrast to the pale blue hydrogel (indicative of less highly cross-linked/fibrillar collagen). Irrespective of CC, BES/CE, or biopolymer, cells with the morphological appearance of macrophages were visible surrounding the hydrogel (and also scattered within the hydrogel) and extending beneath the muscular layer overlying the subcutis.

To confirm the persisting presence of IC-21-Luc macrophages at the implantation site, immunohistochemistry using an anti-luciferase antibody was also performed. Immunostained cells were detected in or around the hydrogel (**Figure 6**), indicating that IC-21-Luc macrophages were still localized to this region.

These studies together with our previous investigations endorse both bio-electrospinning and cell electrospinning as

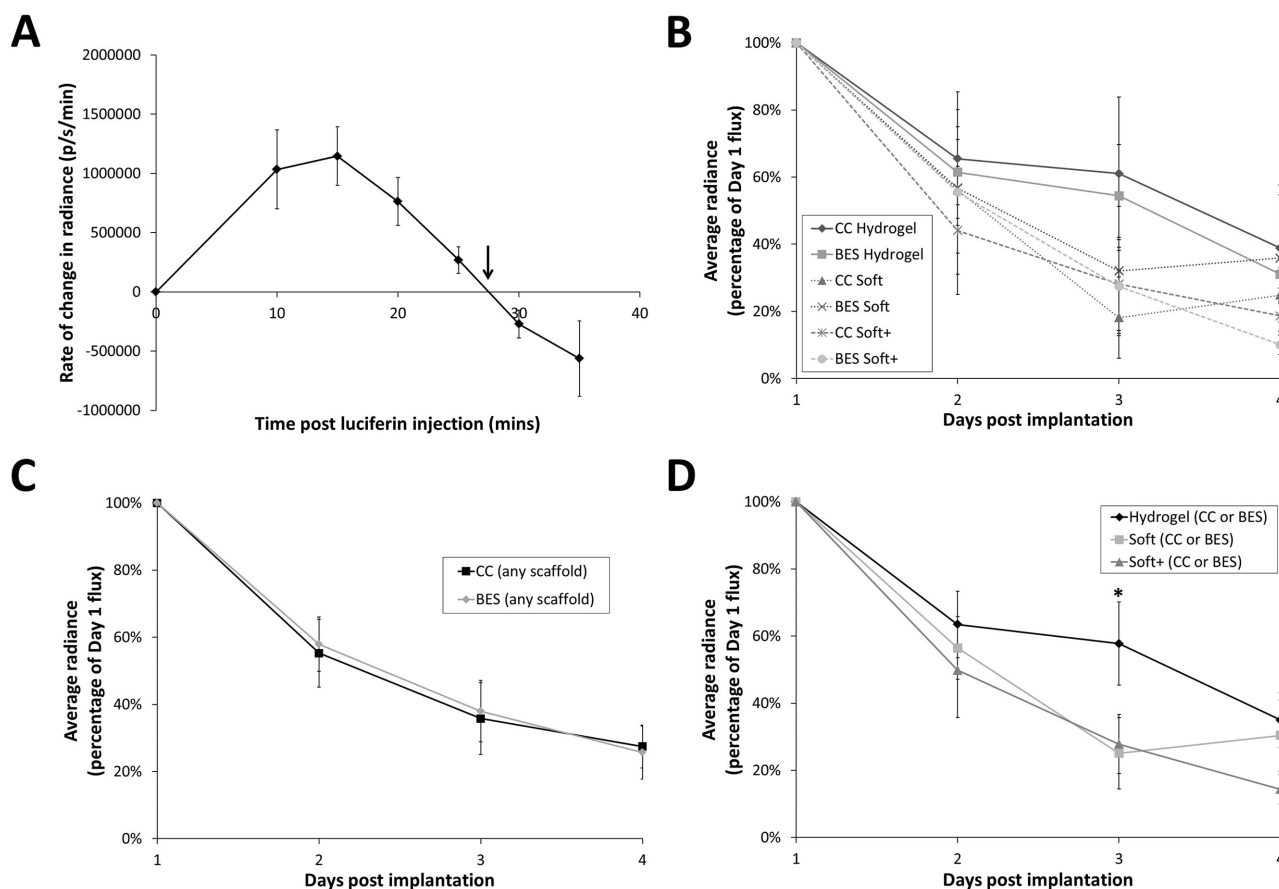


**Figure 3.** Longitudinal bioluminescent image analysis following in vivo macrophage–biopolymer implantation. A) On day 1, a kinetic analysis was performed following injection of D-luciferin to determine the optimal time ( $\approx 25$  min) for identification of peak radiance (when the rate of change of radiance reaches zero), as indicated by an arrow. B) Bioluminescence for each macrophage–biopolymer combination ( $n = 3$  mice per combination) was determined on days 1–4 post-implantation, expressed as a percentage of the peak radiance on day 1. There was a statistically significant decline in signal across all groups over time, but not between groups (two-way repeated measures ANOVA with Holm–Sidak post hoc analysis). C) Analysis of bioluminescence of CC and BES cells (irrespective of biopolymer) indicated an equivalent statistically significant decline in bioluminescence over time. D) Analysis of bioluminescence for the different biopolymers (irrespective of CC/BES) suggests that the standard CollaGel Hydrogel may have higher retention of IC-12-Luc bioluminescent signal than Soft or Soft+ ( $* = p < 0.05$  at day 3; two-way repeated measures ANOVA with Holm–Sidak post hoc analysis).

versatile platform biotechnologies. They have the capacity to directly process living cells in combination with a biopolymer, with the addition of either micro and/or nanomaterials for simultaneously forming complex living 3D architectures or biomaterials for a raft of potential applications in regenerative

medicine. We and others are currently in the process of elucidating the ability to bio-electrospray or cell electrospin cells in a matrix directly into a model organism, so that the technological implications for direct utilization in the clinic are demonstrated.

**Table 1.** Results of two-way repeated measures ANOVA with Holm–Sidak post hoc analysis, examining effect of factor “Time (days post-implantation)” within each treatment (i.e., cell–biopolymer combination).

Comparison	CC Hydrogel	BES Hydrogel	CC Soft	BES Soft	CC Soft+	BES Soft+
Day 1 versus day 2	ns	$p < 0.05$	$p < 0.05$	$p < 0.05$	$p < 0.001$	$p < 0.05$
Day 1 versus day 3	$p < 0.05$	$p < 0.05$	$p < 0.001$	$p < 0.001$	$p < 0.001$	$p < 0.001$
Day 1 versus day 4	$p < 0.001$	$p < 0.001$	$p < 0.001$	$p < 0.001$	$p < 0.001$	$p < 0.001$
Day 2 versus day 3	ns	ns	$p < 0.05$	ns	ns	ns
Day 2 versus day 4	ns	ns	ns	ns	ns	$p < 0.05$
Day 3 versus day 4	ns	ns	ns	ns	ns	ns

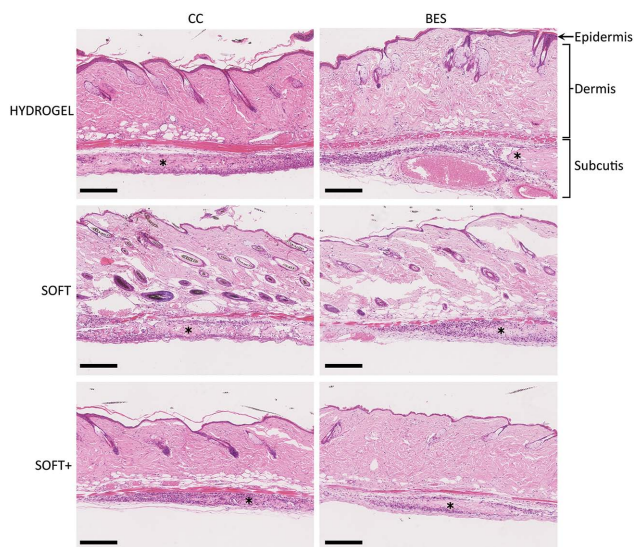


**Figure 4.** Histological analysis of the macrophage–biopolymer implantation site (H&E staining). At day 4 post-implantation, skin was harvested from each dorsal flank, and processed for histology. The various hydrogels (indicated by \*) were discernible within the subcutis. Cells with the morphological appearance of macrophages were visible surrounding the hydrogel, with a scattering of cells within the hydrogel. Scale bar: 200  $\mu\text{m}$ .

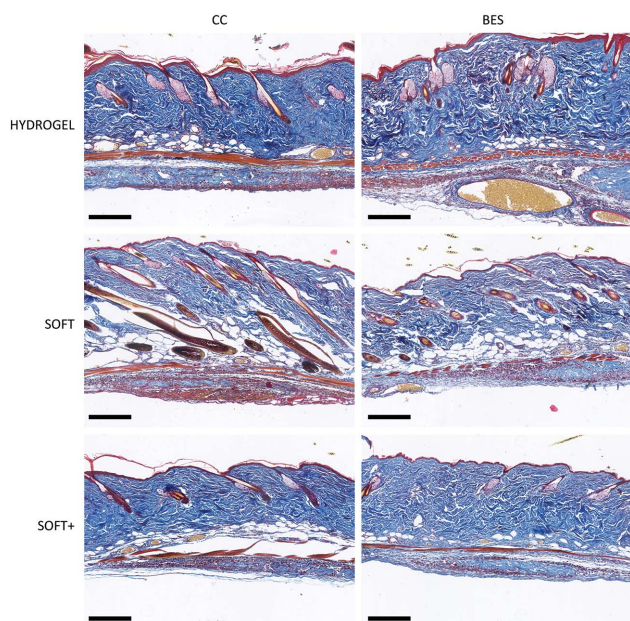


**Figure 5.** Histological analysis of the macrophage–biopolymer implantation site (MSB staining). At day 4 post-implantation, skin was harvested from each dorsal flank, and processed for histology. Where possible, serial sections directly adjacent to those shown in Figure 4 were stained with a modified trichrome stain. Mature fibrillar collagen within the dermis appeared dark blue, while the collagen within the hydrogel was generally lighter blue in appearance, indicating a less highly cross-linked or fibrillar form of collagen. Scale bar: 200  $\mu\text{m}$ .

## Experimental Section

**Cell Culture:** IC-21-Luc were kindly provided by Dr. Katrina McNulty (University College London, London, UK).<sup>[20]</sup> IC-21 cells are

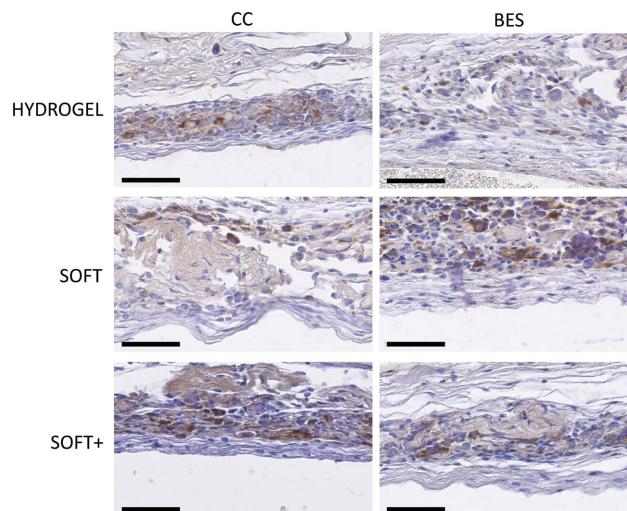


**Figure 6.** Immunolocalization of IC-21-Luc macrophages at the skin implantation site. Immunohistochemistry with an anti-luciferase antibody was used to verify whether cells within or surrounding the hydrogel were IC-21-Luc macrophages expressing this gene. The presence of luciferase immunolocalized (brown staining) to the intracellular compartment of cells with the morphological appearance of macrophages, in the same subcutaneous region as the hydrogel. Scale bar: 50  $\mu\text{m}$ .

an SV40-transformed peritoneal macrophage cell line derived from the C57Bl/6 mouse, and were obtained from the American Type Culture Collection. IC-21s stably expressing luciferase were generated by lentiviral transduction, using a lentiviral vector plasmid pLenti-CMV-Puro-Luc from Dr. E. Campeau, University of Massachusetts Medical School (purchased through Addgene Inc., MA, USA; Vector No. 17477).<sup>[21]</sup> This vector constitutively expresses firefly luciferase under the control of a CMV promoter, and also has a gene for puromycin resistance.

IC-21-Luc cells were grown in RPMI 1640 supplemented with 10% (v/v) fetal bovine serum (FBS), L-glutamine ( $2 \times 10^{-3}$  M), and antibiotics (50 IU mL<sup>-1</sup> penicillin and 50  $\mu\text{g}$  mL<sup>-1</sup> streptomycin; all from Life Technologies, UK), at 37 °C/5% CO<sub>2</sub> in a humidified atmosphere. Cells were passaged using nonenzymatic cell dissociation buffer (Life Technologies, UK), according to the manufacturer's recommendations. IC21-Luc cells were grown in media containing 2  $\mu\text{g}$  mL<sup>-1</sup> puromycin for at least one week during expansion to select for luciferase-transduced cells. Harvested macrophages were initially split into three equal aliquots: (1) untreated CC, (2) cells subsequently subjected to BES, and (3) cells subsequently exposed to CE.

**Bio-Electrospinning and Cell Electrospinning:** Cells were handled using either a single needle bio-electrospray setup or a coaxial cell electrospinning needle system. Both these needle systems have previously been described elsewhere.<sup>[10a,12]</sup> Briefly, the single needle bio-electrospray setup had an internal bore diameter of  $\approx 800$   $\mu\text{m}$  with a wall thickness of  $\approx 700$   $\mu\text{m}$  with the ground electrode placed  $\approx 10$  mm below the needle thus giving rise to an electric field between 0.5 and 1.5 kV mm<sup>-1</sup> over an applied voltage range of 5–15 kV. The coaxial cell electrospinning needle explored in these studies had an inner bore diameter of the inner needle of  $\approx 700$   $\mu\text{m}$  while the outer needle had an inner bore diameter of 1900  $\mu\text{m}$  with a wall thickness of  $\approx 800$   $\mu\text{m}$ . During these cell electrospinning studies a grounded mesh electrode was maintained at a distance of about 15 mm below the needle system, giving rise to an electric field ranging from 0.33 to 0.66 kV mm<sup>-1</sup> for an applied voltage range from 5 to 10 kV. Both systems were housed in a class II laminar flow hood to maintain sterility.

**Flow Cytometry Assessment of Cell Viability:** Flow cytometry was used to assess the viability of post-BES/CE cells in comparison to controls (CC). Cells were collected at 0, 24, 48, and 72 h after bio-electrospraying or cell electrospinning and incubated at room temperature for  $\approx 15$  min

in Annexin V buffer containing  $1.8 \times 10^{-3}$  M calcium,  $4 \mu\text{L mL}^{-1}$  FITC-labeled Annexin V (Pharmingen, UK), and  $5 \mu\text{g mL}^{-1}$  PI (Sigma, UK). Annexin V and PI stain those cells undergoing apoptosis/cell death, by binding to phosphatidylserine in the cell membrane, or to cellular DNA, respectively—and this binding can be visualized by way of flow cytometry. Thus, labeled samples were immediately analyzed using flow cytometry (Becton Dickinson LSR II; BD Biosciences, Oxford, UK), with  $>20\,000$  events collected for each sample. In parallel, unlabelled cells at these time points were morphologically examined by standard phase contrast light microscopy (Leica MZ10, Leica Microsystems, UK).

**Biopolymers Used in These Studies:** Three different rat-tail collagen-based hydrogels were investigated in these studies. These hydrogels were provided by Olaf Pharmaceuticals. They were (a) CollaGel Hydrogel, (b) CollaGel Hydrogel Soft, and (c) CollaGel Hydrogel Soft+. CollaGel Hydrogel Soft contains a less rigid and more porous matrix than regular CollaGel Hydrogel and Soft + contains additives for enhanced growth and attachment. All three of these hydrogels are a biocompatible complex of Type I Collagen fibers. These hydrogels contain a high quality, sterile Type I Rat Tendon Collagen that has been specially formulated for ease of gel formation. A useful feature for the current studies is that these gels both could be made to free flow and also gels once injected into mice. Additionally, the gels have a reasonable ability to withstand stretching without tearing. For cell electrospinning studies these gels were further modified by mixing in concentrated laminin to increase their viscoelasticity so that they could be cell electrospun in stable conditions.

**Bioluminescent Imaging of Mice:** Male C57BL/6 mice (Charles River, UK) were housed in a specific pathogen-free facility, and all procedures were performed on mice between 12 and 15 weeks of age ( $n = 3$  per group). All animal studies were ethically approved and licensed under the UK Home Office Animals (Scientific Procedures) Act 1986. Under light isoflurane-induced anesthesia, the dorsal flanks of each mouse were shaved and sterilized.  $3 \times 10^6$  untreated IC21-Luc cells (CC) or those subjected to BES or CE were mixed 1:1 (v/v) with the respective biopolymers: (a) CollaGel Hydrogel, (b) CollaGel Hydrogel Soft, or (c) CollaGel Hydrogel Soft+. A total volume of  $100 \mu\text{L}$  of the particular hydrogel/cell mix was then injected subcutaneously into the dorsal flank (with CC on the left side and BES on the right side of each mouse), and allowed to gel.

On days 1–4 post-injection,  $150 \mu\text{L}$  of D-luciferin substrate ( $10 \text{ mg mL}^{-1}$ ; Regis Technologies Inc., USA) was given by intraperitoneal injection prior to imaging. For imaging, mice were anesthetized in an induction chamber using isoflurane and then transferred to the imaging chamber of an IVIS Lumina II imaging system (Caliper Life Sciences, UK) where they were maintained on isoflurane anesthesia via nose cones, and kept on a heated mat to maintain body temperature. On each of days 1–4 post-injection, luminescent images were acquired with an exposure time of 5 min,  $24 \times 24 \text{ cm}$  field of view, medium binning (factor 4), and f stop 1.2, starting from 15 min after the luciferin injection, to enable empirical determination of imaging during the plateau phase of bioluminescence.

**Bioluminescent Image Analysis:** Images were analyzed using Living Image 3.2 software (Caliper Life Sciences, UK) to generate pseudo-color scaled images overlaid on greyscale images, providing 2D localization of the luminescent light source. Identically sized  $2.0 \times 1.3 \text{ cm}$  regions of interest (ROI) were drawn using shape tools and the light emission (peak radiance) within each ROI (placed above the left and right dorsal flank) was quantified in photons per second, during the plateau phase of bioluminescence.

**Tissue Harvesting, Histological and Immunohistochemical Analysis:** Animals were sacrificed 4 d following cell transfer, and skin encompassing the transfer site was dissected out, fixed in 4% paraformaldehyde for 24 h, and then dehydrated through ethanol prior to embedding in a transverse orientation in paraffin wax. For subsequent analysis, 2–5  $\mu\text{m}$  sections were then cut and stained with standard H&E staining, or a modified trichrome (Martius Scarlet Blue [MSB]) stain for collagen, using an automated Sakura Tissue-Tek DRS 2000 Multiple Slide Stainer.

For luciferase immunohistochemistry, sections were dewaxed, antigens retrieved using standard citrate treatment, washed and then

incubated with 3% hydrogen peroxide for 30 min to block endogenous peroxidase activity. Sections were blocked with a solution of 1:6 (v/v) goat serum in TBS with avidin block (Avidin/Biotin Blocking Kit, Vector Laboratories, Burlingame, USA) for 20 min, and then incubated overnight at  $4 \text{ }^\circ\text{C}$  with a rabbit polyclonal anti-firefly luciferase antibody (1:2000 dilution; Abcam, UK) in TBS with 1% BSA, 1% goat serum, and biotin block (Avidin/Biotin Blocking Kit, Vector Laboratories, Burlingame, USA). After washing, sections were incubated for 1 h with biotinylated goat anti-rabbit IgG (diluted 1:200 in TBS with 1% BSA). After three further washes, sections were incubated for 30 min with streptavidin-conjugated horseradish peroxidase (Invitrogen, Paisley, UK) diluted 1:200 in TBS. Sections were washed and incubated with DAB Peroxidase Substrate Kit (Vector Labs, Burlingame, USA) for 10 min, followed by counterstaining with Gill-2 hematoxylin (Thermo Shandon, USA).

All sections were subsequently scanned on a Nanosizer and images were captured using NDP view software (both from Hamamatsu Corporation, Hamamatsu, Japan).

## Acknowledgements

S.N.J. thankfully acknowledges The Royal Society (UK) and the National Institutes of Health (USA) for funding the BioPhysics Group at UCL. C.J.S. was supported by an MRC Career Development Award (G0800340). The authors wish to thank Dr. Jamie Wilson and Mr. Bartłomiej Marcinowski at Olaf Pharmaceuticals for all their assistance with the design and supply of the hydrogel samples.

Received: June 22, 2015

Revised: September 2, 2015

Published online: October 28, 2015

- [1] L. Rayleigh, *Philos. Mag.* **1882**, *14*, 184.
- [2] a) J. F. Cooley, *US Patent* 692,631, **1902**; b) W. J. Morton, *US Patent* 705,691, **1902**.
- [3] a) S. Sundarrajan, K. L. Tan, S. H. Lim, S. Ramakrishna, *Proc. Eng.* **2014**, *75*, 159; b) J. A. Tapia-Hernández, P. I. Torres-Chávez, B. Ramírez-Wong, A. Rascón-Chu, M. Plascencia-Jatomea, C. G. Barreras-Urbina, N. A. Rangel-Vázquez, F. Rodríguez-Félix, *J. Agric. Food Chem.* **2015**, *63*, 4699; c) A. G. Bailey, *Electrostatic Spraying of Liquids*, Research Studies Press, Ltd., Taunton, UK **1988**.
- [4] S. N. Jayasinghe, *Analyst* **2011**, *136*, 878.
- [5] a) J. B. Fenn, M. Mann, C. K. Meng, S. F. Wong, C. M. Whitehouse, *Science* **1989**, *246*, 64; b) R. Sridhar, R. Lakshminarayanan, K. Madhaiyan, V. A. Barathi, K. H. C. Lim, S. Ramakrishna, *Chem. Soc. Rev.* **2015**, *44*, 790.
- [6] S. N. Jayasinghe, *Analyst* **2013**, *138*, 2215.
- [7] C. A. E. Hamlett, S. N. Jayasinghe, J. A. Preece, *Tetrahedron* **2008**, *64*, 8476.
- [8] S. Irvine, A. C. Sullivan, J. R. McEwan, S. N. Jayasinghe, *Biotechnol. J.* **2008**, *3*, 124.
- [9] D. J. Gilmartin, M. M. Alexaline, C. Thrasivoulou, A. R. Phillips, S. N. Jayasinghe, D. L. Becker, *Adv. Healthcare Mater.* **2013**, *2*, 1151.
- [10] a) S. N. Jayasinghe, A. N. Qureshi, P. A. M. Eagles, *Small* **2006**, *2*, 216; b) S. N. Jayasinghe, A. Townsend-Nicholson, *Lab Chip* **2006**, *6*, 1086.
- [11] A. Townsend-Nicholson, S. N. Jayasinghe, *Biomacromolecules* **2006**, *7*, 3364.
- [12] S. N. Jayasinghe, S. Irvine, J. R. McEwan, *Nanomedicine* **2007**, *2*, 555.
- [13] a) V. L. Workman, L. B. Tezera, P. T. Elkington, S. N. Jayasinghe, *Adv. Funct. Mater.* **2014**, *24*, 2648; b) B. Al shammary, T. Shiomi, L. Tezera, M. K. Bielecka, V. Workman, T. Sathyamoorthy, F. Mauri, S. N. Jayasinghe, B. D. Robertson, J. D'Amiento, J. S. Friedland, P. T. Elkington, *J. Infect. Dis.* **2015**, *212*, 463.

- [14] a) N. Andreu, D. Thomas, L. Saraiva, N. Ward, K. Gustafsson, S. N. Jayasinghe, B. D. Robertson, *Small* **2012**, *8*, 2495; b) S. Sampson, L. Saraiva, K. Gustafsson, S. N. Jayasinghe, B. D. Robertson, *Small* **2014**, *10*, 78.
- [15] a) A. S. Patel, A. Smith, R. Q. Attia, O. Lyons, P. Saha, B. Modarai, S. N. Jayasinghe, *Integr. Biol.* **2012**, *4*, 628; b) S. P. Barry, S. N. Jayasinghe, D. S. Latchman, A. Stephanou, *BioProcess. J.* **2007**, *6*, 8.
- [16] a) H. Kempfski, N. Austin, A. Roe, S. Chatters, S. N. Jayasinghe, *Regener. Med.* **2008**, *3*, 343; b) S. N. Jayasinghe, G. Warnes, C. Scotton, *Macromol. Biosci.* **2011**, *11*, 1364.
- [17] K. Bartolovic, N. Mongkoldhumrongkul, S. N. Waddington, S. N. Jayasinghe, S. J. Howe, *Analyst* **2010**, *135*, 157.
- [18] a) J. D. W. Clark, S. N. Jayasinghe, *Biomed. Mater.* **2008**, *3*, 011001; b) T. Geach, N. Mongkoldhumrongkul, L. B. Zimmerman, S. N. Jayasinghe, *Analyst* **2009**, *134*, 743; c) P. Joly, B. Hennings, S. N. Jayasinghe, *Biomicrofluidics* **2009**, *3*, 044107; d) N. Mongkoldhumrongkul, S. C. Swain, S. N. Jayasinghe, S. Stürzenbaum, *J. R. Soc., Interface* **2010**, *7*, 595; e) N. K. Pakes, S. N. Jayasinghe, R. S. B. Williams, *J. R. Soc., Interface* **2011**, *8*, 1185.
- [19] E. A. Phelps, A. J. García, *Curr. Opin. Biotechnol.* **2010**, *21*, 704.
- [20] K. McNulty, E. K. Sage, R. Alexander, C. J. Scotton, S. M. Janes, *Thorax* **2012**, *67* (Suppl. 2), A62.
- [21] E. Campeau, V. E. Ruhl, F. Rodier, C. L. Smith, B. L. Rahmberg, J. O. Fuss, J. Campisi, P. K. Cooper, P. D. Kaufman, *PLoS One* **2009**, *6*, e6529.